Schizosaccharomyces pombe Ras1 Effector, Scd1, Interacts With Klp5 and Klp6 Kinesins to Mediate Cytokinesis

Yingchun Li and Eric C. Chang[1]

Baylor College of Medicine, Department of Molecular and Cellular Biology, The Breast Center, Methodist Hospital, Houston, Texas 77030

Manuscript received March 14, 2003
Accepted for publication June 6, 2003

ABSTRACT

Fission yeast Scd1 is an exchange factor for Cdc42 and an effector of Ras1. In a screen for *scd1* interacting genes, we isolated *klp5* and *klp6*, which encode presumptive kinesins. Klp5 and Klp6 form a complex to control the same processes, which so far include microtubule dynamics and chromosome segregation. We showed that *klp5* or *klp6* inactivation in combination with the *scd1* deletion (*scd1*Δ) created a synthetic temperature-dependent growth defect. Further genetic analysis demonstrated that Klp5 and Klp6 interacted specifically with the Ras1-Scd1 pathway, but not with the Ras1-Byr2 pathway. In addition, Klp5 and Klp6 can stably associate with Scd1 and Cdc42. A deletion in the Scd1 C terminus, which contains the PB1 domain, prevented Scd1 binding to Klp5/6 and caused a growth defect in Klp5/6 mutant cells that is indistinguishable from that induced by *scd1*Δ. Analysis of the double-mutant phenotype indicated that at the nonpermissive temperature, cells failed to undergo cytokinesis efficiently. These cells contained abnormal contractile rings in which F-actin and Mid1, a key regulator of F-actin ring formation and positioning, are mispositioned and fragmented. These data suggest that Klp5/6 cooperate with the Ras1-Scd1 pathway to influence proper formation of the contractile ring for cytokinesis.

SCHIZOSACCHAROMYCES pombe has a single homolog of the human H-Ras protooncoprotein, called Ras1 (Fukui and Kaziro 1985). Ras1 activates the Byr2 protein kinase to regulate gene expression that is crucial for sexual differentiation (Wang *et al.* 1991; Chang *et al.* 1994). Ras1 also regulates Scd1/Ral1, which is a putative guanine nucleotide exchange factor (Fukui and Yamamoto 1988; Chang *et al.* 1994) for Cdc42, a member of the Rho family of Ras-like proteins, and Cdc42, in turn, activates the Shk1/Orb2 protein kinase (Verde *et al.* 1998). The Ras1-Scd1 pathway is further regulated by a scaffold protein, Scd2/Ral3, which positively affects protein binding between components in this pathway (Chang *et al.* 1994, 1999).

Scd1 is localized to cell ends, the cell equator, the nucleus, and the spindle (Li *et al.* 2000). Since overexpression of a dominant negative Cdc42 (Cdc42T17N) reduces the amount of nuclear Scd1 while concomitantly increasing the amount of Scd1 at the cell ends, Scd1 seems to move between the cell cortex and the nucleus. The dynamic localization of Scd1 suggests that the Ras1-Scd1 pathway in *S. pombe* can engage in a wide variety of activities such as the regulation of cell polarity and spindle functioning, as well as cytokinesis.

Since one of the best-documented conserved functions of the Ras and Rho-like proteins is the control of cytoskeleton functioning (Van Aelst and D'Souza-Schorey 1997), it is highly probable that the *S. pombe* Ras1-Scd1 pathway can control cellular activities by similarly interacting with cytoskeleton components. Intriguingly, while the Ras pathways in fibroblasts and budding yeast can regulate functioning of the actin cytoskeleton, we and others have found that the Ras1-Scd1 pathway can also affect the functioning of microtubules in *S. pombe*. For example, we have demonstrated that Scd1 colocalizes with the spindle; furthermore, mutations that inactivate the Ras1-scd1 pathway, together with tubulin mutations, block proper spindle formation (Li *et al.* 2000). Furthermore, inactivation of the Ras1-Scd1 pathway renders cells hypersensitive to TBZ (thiabendazole) and MBC (methyl benzimidazolecarbamate), both of which promote microtubule depolymerization (Li *et al.* 2000; Qyang *et al.* 2002), and is synthetically lethal with the deletion of *tea1* (Papadaki *et al.* 2002; Qyang *et al.* 2002), which encodes a microtubule-binding protein that was first discovered as a key regulator for cell polarity (Mata and Nurse 1997). Cells defective in both Tea1 and the Ras1-Scd1 pathway show abnormalities in polarity, chromosome segregation, and cytokinesis.

To further investigate the relationship between the Ras1 pathway and microtubules, we performed a genetic screen seeking chromosomal suppressors (named *sot*, *s*uppressors *o*f *T*BZ sensitivity) that rescue the TBZ hypersensitivity of *scd1*Δ cells. Among these suppressors, we further selected those that act synergistically with *scd1*Δ to affect cell growth. In this study, we report the

[1]*Corresponding author:* 1 Baylor Plaza, Baylor College of Medicine, Department of Molecular and Cellular Biology, The Breast Cancer Center, Methodist Hospital, BCM 600, Houston, TX.
E-mail: echang@breastcenter.tmc.edu

isolation of *sot1* and *sot2*, which encode Klp5 and Klp6 that belong to the Kip3 family of kinesin (plus-end) motor proteins (West *et al.* 2001). Klp5 and Klp6 are not essential for cell division, and the only major mitotic abnormality noted in the null mutants is a transient defect in chromosome segregation, which results in the appearance of lagging chromosomes in early anaphase (Garcia *et al.* 2002a,b; West *et al.* 2002). The phenotypes of *klp5*Δ and *klp6*Δ cells in these studies were reported to be nearly indistinguishable; furthermore, Klp5 and Klp6 form a complex in *S. pombe* cells (Garcia *et al.* 2002b). These data are consistent with the hypothesis that Klp5 and Klp6 can participate in the same biological process. It is not clear whether Klp5 and Klp6 have functions in addition to regulation of chromosome segregation.

In this study, we show that Scd1, as well as Cdc42, binds stably with Klp5 and Klp6. Surprisingly, however, our data suggest that when both the Ras1-Scd1 pathway and the Klp5/6 complex are inactivated, the cells lose viability due to cytokinesis abnormality, but not chromosome missegregation. These mutant cells display severe defects in contractile ring formation as their F-actin and Mid1, a key regulator for F-actin ring formation (Chang *et al.* 1996; Sohrmann *et al.* 1996; Bähler *et al.* 1998a; Paoletti and Chang 2000), are fragmented and/or misplaced in the cell cortex during mitosis. These results support a model in which the Ras1-Scd1 pathway can interact with Klp5/6 to influence the proper formation of the contractile ring for cytokinesis.

MATERIALS AND METHODS

Parental strains and growth conditions: The generic wild-type strain is SP870 (*h*^{90}, *ade6-M210, leu1-32, ura4-D18*). Strains SPRU (*ras1::ura4*), SPSCD2L (*scd2::LEU2*), SPSL (*byr2::LEU2*), and SPSCD1U (*scd1::ura4*) were all derived from SP870 as described (Wang *et al.* 1991; Chang *et al.* 1994). Strain SP42N17 (Marcus *et al.* 1995), containing an integrated plasmid expressing the dominant negative Cdc42T17N, is from S. Marcus (University of Texas, M. D. Anderson Cancer Center, Houston). Strain YDM296, containing the temperature-sensitive *mid1-18* mutation, and strain YDM603, containing a Mid1 tagged at its C terminus with 13 copies of the cMYC epitope, are from D. McCollum (University of Massachusetts Medical Center, Boston; Bähler *et al.* 1998a). The *shk1/orb2-34* mutant is from F. Verde (University of Miami School of Medicine, Miami; Verde *et al.* 1998). *S. pombe* cells were cultured in either rich medium yeast extract adenine uracil (YEAU) or synthetic minimal medium (MM; Alfa *et al.* 1993). To examine phenotypes of mutants at the nonpermissive temperature, asynchronized cultures were pregrown at 25° and rediluted into the YEAU medium prewarmed at 35° to 1×10^6 cells/ml. For synchronization in S phase, cells in early log phase (2×10^6 cells/ml) were treated by hydroxyurea (HU; 11 mm) for 3 hr followed by a second dose of HU for one more hour at 25°. These cells were then washed with HU-free medium and resuspended in fresh medium at 35°. Cell viability was assayed by plating for colony formation in the YEAU medium at 25°. For the spotting type of experiments, cells of equal number were serially diluted 1:5 and then spotted on YEAU plates.

Isolation of *sot* mutants: Approximately 4×10^9 *scd1*Δ cells (strain SPSCD1U) were plated in the presence of TBZ at 15 μg/ml, a concentration that prohibits colony formation of *scd1*Δ but not wild-type cells (strain SP870). Forty-four colonies emerged, and of these, 11 were temperature sensitive (Ts), and 1 cold sensitive (Cs). We chose to focus on these 12 clones with temperature-dependent trackable phenotypes that are useful for gene cloning. These 12 mutations were backcrossed and shown to be single and recessive. Complementation analysis determined that the 11 mutations acting in concert with *scd1*Δ to induce a Ts phenotype belong to two complementation groups, *sot1* and *sot2*. There are six members in the *sot1* group, *sot1-1*–*sot1-6*, and five members in the *sot2* group, *sot2-1*–*sot2-5*. All the *sot1* and *sot2* alleles produced phenotypes that were later found to be nearly identical to those induced by the null mutations (see results), indicating that they are all loss-of-function mutations. The remaining mutation, which together with *scd1*Δ produces a Cs phenotype, is in a separate complementation group and was named *sot3-1*.

Isolation of *sot1/klp5* and *sot2/klp6* genes: *scd1*Δ *sot1-1* and *scd1*Δ *sot2-1* strains were used to screen a genomic library (Barbet *et al.* 1992) for clones that rescue the Ts phenotype. Two clones of genes encoding full-length *klp5* were isolated when the *scd1*Δ *sot1-1* strain was used as host. One of them was named pKLP5, which contains the coding region for *klp5* along with 2.1-kb upstream and 3.3-kb downstream regions. When the *scd1*Δ *sot2-1* strain was used as host, nine clones encoding *klp6* were isolated. One of them was named pKLP6, which contains the full-length *klp6* gene plus 0.4-kb upstream and downstream regions. In addition, full-length *scd1* was isolated once in each case, and a truncated *scd1* lacking the coding sequence for the last 150 amino acids was also isolated once during the cloning of the *klp6* gene. The truncated Scd1 was just a weak suppressor, however, which, together with the data presented in this article, suggests that the N terminus plays a more minor role in interacting with Klp6. *klp5*Δ and *klp6*Δ strains were prepared (see below) and they produced the same phenotype as *sot1-1* and *sot2-1* strains. As reported previously (West *et al.* 2001), although these mutants do not have any detectable growth defects, they have an abnormally bent cell shape, typical of cells defective in microtubule cytoskeleton, and are abnormal during meiosis, frequently producing abnormal tetrads. We used these phenotypes to perform standard complementation analysis. Our data indicate that *sot1* mutations are in the same complementation group as *klp5*Δ, while *sot2* mutations and *klp6*Δ are in another complementation group. Furthermore, during tetrad analysis, we did not isolate wild-type cells from *sot1/klp5*Δ cells, indicating that *sot1* and *klp5* are very close to one another in the chromosome. Likewise, *sot2* was determined to be linked to *klp5*. Finally, *klp5* overexpression using pKLP5 rescues the phenotypes of both the *scd1*Δ *sot1-1* strain and the *sot1* single mutants, and *klp6* overexpression using pKLP6 rescues the phenotypes of the *scd1*Δ *sot2-1* strain and the *sot2* single mutants. These genetic results indicate that *sot1* and *sot2* are the same as *klp5* and *klp6*, respectively.

Plasmid constructions: To delete *klp5* and *klp6* genes by one-step gene replacement, knock-out plasmids pKLP5U and pKLP6U were constructed from pKLP5 and pKLP6 (isolated above) as follows: pKLP5U was built by replacing the 1.6-kb *Psh*AI-*Hpa*I fragment from pKLP5 with a *ura4* gene. pKLP6U was built by replacing the 1.9-kb *Eco*RI-*Spe*I fragment from pKLP6 with *ura4*. Because both *klp5* and *klp6* genes have one intron at the 5′ end of the gene, full-length cDNAs for both genes were constructed by first amplifying the 5′ part of the open reading frame (ORF) using PCR and then fusing them with the 3′ part of the ORF, obtained from the genomic DNA. Specifically, the first 0.8-kb fragment of the *klp5* cDNA and

0.6 kb of the *klp6* cDNA were amplified by PCR primers containing a *Bam*HI site. These PCR products were cloned into pBluescript II S/K− (Stratagene, La Jolla, CA) to obtain pBS-KLP5N and pBS-KLP6N. Both cDNA fragments were sequenced. Next, the 3′ part of the *klp5* ORF was released from pKLP5 as a *Sph*I-*Kpn*I fragment whose *Kpn*I site was blunt ended. This fragment was cloned into the *Sph*I/*Hinc*II sites in pUC119 to obtain pUC119-KLP5C. Similarly, a 2.4-kb *Eco*RI-*Stu*I fragment encoding the C-terminal portion of Klp6 was cloned from pKLP6 into the *Eco*RI-*Sma*I sites of pUC119 to obtain pUC119-KLP6C. Finally, a 0.8-kb *Bam*HI-*Sph*I fragment from pBS-KLP5N and a 2.3-kb *Sph*I-*Bam*HI fragment from pUC119-KLP5C were cloned into the *Bam*HI site of pREP-41GFP (Chen *et al.* 1999), pGADGH (Chang *et al.* 1994), and pVJL11 (Chang *et al.* 1994) and into the *Bgl*II site of pSLF173 (Forsburg and Sherman 1997) to construct pREP41GFP-KLP5, pGADKLP5, pLBDKLP5, and pSLF173-KLP5, respectively. Similarly, a 158-bp *Bam*HI-*Eco*RI fragment from pBS-KLP6N and a 2.4-kb *Eco*RI-*Bam*HI fragment from pUC119-KLP6C were ligated to the same set of vectors to construct pREP41GFP-KLP6, pGADKLP6, pLBDKLP6, and pSLF173-KLP6. pAD-MID1 was modified from pJG4-5PL-Mid1 (Bähler *et al.* 1998a) by disrupting the original *TRP1* marker with *LEU2*. pAD was constructed as a control vector for the two-hybrid assay by first removing *mid1* from pJG4-5PL-Mid1 and then by disrupting *TRP1* with *LEU2*. A *Bam*HI fragment of *scd1* lacking the last 58 bp of the coding sequence was cloned from pGADSCD1ΔB (Chang *et al.* 1994) into pALG (Li *et al.* 2000) and pVJL11 to construct pALGSCD1ΔB and pLBDSCD1ΔB. A coding region for the 3′ end of *scd1* was obtained from pGADSCD1 (Chang *et al.* 1994) by an *Apa*I digestion and then blunt ended and finally cut with *Sac*I. This fragment was cloned into the *Sac*I-*Sal*I (*Sal*I site was blunt ended) site in pLBDSCD1ΔB to create pLBDSCD1. A DNA fragment encoding the C-terminal 163 amino acids of Scd1 (Scd1ΔN) was released from pHTSCD1ΔN (Chang *et al.* 1994) by *Nhe*I, blunt ended, and finally digested with *Bgl*II. The resulting fragment was inserted into pVJL11 to create pLBDSCD1ΔN. To express Scd1-GFP, we first constructed pCGFP as follows: EGFP was modified by PCR to harbor a *Bam*HI and *Sma*I site to allow this to be subcloned into pREP1. *scd1* cDNA was amplified and modified by PCR as a *Sal*I-*Bgl*II fragment to allow cloning into pCGFP to create pREP1SCD1GFP. *scd1* was excised from pALGSCD1 (Li *et al.* 2000) and cloned into pSLF173 and pAAUGST (Gilbreth *et al.* 1996) to obtain pSLFSCD1 and pAAU-GSTSCD1. To express GST-Scd1 under the *nmt1* promoter, a DNA fragment encoding the GST-Scd1 was released from pAAU-GSTSCD1 and cloned into pREP1 to construct pREP1-GSTSCD1. A *Pst*I-*Sac*I fragment from pAAUGST containing the coding sequence of glutathione S-transferase (GST) was inserted into pART1 to create the control plasmid pART1-GST. pAAU-GSTCDC42 and pAAU-GSTCDC42V12 were constructed by cloning a *Sal*I-*Sac*I fragment from pALUCDC42SP (Chang *et al.* 1994) or pREP1-CDC42V12 (S. Marcus, M. D. Anderson Cancer Center) into pAAUGST.

Gene deletion and tagging: Strain SP870 was transformed with a *Pst*I-*Sma*I fragment released from pSCD1L (Li *et al.* 2000) to generate the SCD1L (*scd1::LEU2*) strain. To delete *klp5* and *klp6*, the 4.6-kb *Bgl*II-*Kpn*I fragment from pKLP5U and the 3-kb *Hpa*I fragment from pKLP6U were used to transform SP870 at 25° to create strains KLP5U (*klp5::ura4*) and KLP6U (*klp6::ura4*), respectively. This results in the deletion of the coding sequence for the N-terminal 520 amino acids of Klp5 and for amino acid residues 53–681 of Klp6. Both knock-outs remove the motor domain. Similarly, *klp5* and *klp6* were deleted from strain SCD1L to construct double null strains S1LK5U (*scd1::LEU2 klp5::ura4*) and S1LK6U (*scd1::LEU2 klp6::ura4*). Proper gene deletions were confirmed by colony PCR (http://www.bio.uva.nl/pombe/handbook). Strains KLP5A (*klp5::ura4::ADE2*), S1LK5A (*scd1::LEU2 klp5::ura4::ADE2*), and S1LK6A (*scd1::LEU2 klp6::ura4::ADE2*) were obtained by transforming strains KLP5U, S1LK5U, and S1LK6U with a *Not*I-linearized pVINPSTnmt81 (*ADE2*$^+$; Kim *et al.* 2001) to replace *ura4* with *ADE2*. Strain KLP5A was fused with strains KLP6U and S1LK6U to create diploids. Their tetrads were dissected to obtain double-mutant K5AK6U (*klp5*Δ *klp6*Δ) and triple-mutant S1LK5AK6U (*scd1*Δ *klp5*Δ *klp6*Δ). Strain KLP5U was fused with strains SPSCD2L, SPSL, and SP42N17 and tetrads were dissected to select strains S2LKP5U (*scd2*Δ *klp5*Δ), B2LK5U (*byr2*Δ *klp5*Δ), and K5U42T17N (*cdc42T17N* overexpression in *klp5*Δ cells), respectively. Double-mutant R1UK5A (*ras1*Δ *klp5*Δ) was built by fusing strains SPRU with KLP5A followed by tetrad dissection. Tagging strains YC1 (*scd1-13MYC*) and YC2 (*scd1*Δ*B-13MYC*) were obtained by a PCR-based method using pFA6a-13Myc-kanMX6 as template (Bähler *et al.* 1998b). In the latter strain, the coding sequence for the 13× cMYC epitope followed by a stop codon was inserted into the coding sequence for amino acid residue 853 of Scd1. Strain SP870 was transformed with the PCR products, and stable G418 colonies were selected. Proper tagging was verified by PCR and Western blot. Strain YC2 (*scd1*Δ*B-13MYC*) was fused with strains YDM296 and KLP5A to eventually create strains YC3 and YC4, which carry *mid1-18 scd1*Δ*B* and *klp5*Δ *scd1*Δ*B*, respectively. Strain SPSCD1U was fused with strain YDM296 to create strain YC5, which carries both *scd1*Δ and *mid1-18*. The Mid1-13Myc tagging strain YDM603 was fused to the double mutant carrying *scd1*Δ *sot1-1* to create Mid1-13Myc tagging strains in the genetic background of *scd1*Δ, *sot1-1*, and *scd1*Δ *sot1-1*. These strains were named YC6, YC7, and YC8, respectively. Similarly, we constructed strains YC9 and YC10 carrying Mid1-13Myc with *klp5*Δ and *scd1*Δ *klp5*Δ, respectively.

Fluorescence microscopy: For GFP-Klp5 and GFP-Klp6 imaging, cells transformed with pREP41GFP-KLP5 or pREP41-GFP-KLP6 were grown in MM medium without thiamine. Under this condition, the expression level of Klp5 and Klp6 is not toxic to the cells. To document GFP-Scd1 and GFP-Scd1ΔB expressed under the control of the strong *adh1* promoter, cells were examined as soon as colonies emerged after transformation (Li *et al.* 2000). To examine Scd1-GFP expressed from the *nmt1* promoter, transformed cells were first grown in MM containing 2 μM thiamine and then were cultured in medium with 0.25 μM thiamine. To study whether disrupting microtubules and F-actin can affect protein localization, cells were first pregrown on plates and then resuspended in medium containing 25 μg/ml MBC or 10 μM latrunculin (LatA). For microtubule staining using the TAT1 antibody, cells were fixed either with methanol at −20° for at least 10 min or with both 3% paraformaldehyde and 0.05% glutaraldehyde for 90 min. To stain Mid1-13Myc using the 9E10 antibody, cells were fixed with 4% formaldehyde for 30 min (Bähler *et al.* 1998a). To stain F-actin, cells were fixed in 3.7% formaldehyde for 30 min and then stained by 20 units/ml rhodamine-conjugated phalloidin. To visualize the septum, cells were fixed in 3.7% formaldehyde for 10 min and stained with calcofluor. DNA was stained by 4′,6-diamidino-2-phenylindole.

Yeast two-hybrid analysis: The reporter strain used was L40, which carries the reporter genes *lexA-lacZ* and *lexA-HIS3* (Vojtek *et al.* 1993). The β-galactosidase activity was measured using a color filter method and the *HIS3* activity was measured by plating cells in medium lacking histidine (Chang *et al.* 1994). The activation domain hybrid proteins were generated by the fusion to either GAL4 or B42. The DNA-binding domain hybrid proteins were constructed by fusion to LexA.

GST pull-down assays: Cells (SP870) were transformed with pREP1-GSTSCD1 and then seeded in the presence of 20 μM

thiamine. These cells were inoculated into the 500 ml thiamine-free medium and grown for 24 hr to log phase. The harvested cells were broken by a French press in 140 ml low-salt RIPA buffer [50 mm Tris, pH 8.0, 1% NP40, 0.5% DOC, 0.1% SDS, 1 mm dithiothreitol (DTT), and a protease inhibitors cocktail]. To make lysate containing GST-Cdc42 and GST-Cdc42V12, cells transformed with pAAU-GSTCDC42 and pAAU-GSTCDC42V12 were grown in thiamine-free medium to log phase and then broken by glass beads in the PEM buffer (Alfa *et al.* 1993) supplemented with 0.5% NP40, 1 mm DTT, and a protease inhibitors cocktail. After centrifugation ($3000 \times g$, 15 min), GST fusion proteins in the supernatant were captured by glutathione beads, which were then incubated with lysates containing HA-Klp5 or HA-Klp6. These lysates were made from cells carrying pSLF173-KLP5 or pSLF173-KLP6, respectively. These cells were pregrown for 20 hr in thiamine-free medium and lysates were made with the same PEM-based lysis buffer. After washing, proteins bound to the GST fusion proteins were resolved by SDS-PAGE and Western blot analysis.

Western blot analysis: For proteins that are tagged with hemagglutinin (HA), c-Myc, GST, or green fluorescent protein (GFP), 12CA5 (1:500), 9E10 (1:500), and commercial goat anti-GST antibody (1:2000, Amersham Pharmacia Biotech, Piscataway, NJ) were used as primary antibodies. Tubulins were detected by TAT1 (Chen *et al.* 1999).

RESULTS

Cloning of *sot1/klp5* and *sot2/klp6* genes: To identify microtubule-binding proteins that interact with Scd1, we first searched for spontaneous recessive mutations that can rescue the hypersensitivity of *scd1*Δ cells to a microtubule-depolymerizing drug, TBZ (Figure 1A). We then focused on those mutations that act cooperatively with *scd1*Δ to produce a growth defect that is either undetectable or weak in the single mutants. Mutations in three genes, *sot1*, *sot2*, and *sot3*, were thus identified (materials and methods). *scd1*Δ in combination with either the *sot1* or the *sot2* mutations creates a Ts growth defect (Figure 1A), while *scd1*Δ, together with the *sot3* mutation, creates a Cs growth defect (our unpublished results).

The Ts growth defects of *scd1*Δ *sot1*$^-$ and *scd1*Δ *sot2*$^-$ strains were used to screen a genomic library for *sot1* and *sot2* genes (see materials and methods). Our results show that *sot1* and *sot2* are the recently identified *klp5* and *klp6* genes, respectively, which encode heavy chains of members of the kinesin motor protein family (West *et al.* 2001).

Deletion mutants of *klp5* and *klp6*, like the *sot1* and *sot2* mutants, are viable and do not display any detectable growth defects at 35° (Figure 1A; West *et al.* 2001). To further investigate the genetic interactions among Scd1 and Klp5 and Klp6, we created *scd1*Δ *klp5*Δ and *scd1*Δ *klp6*Δ double null mutants and found that these double null mutants also fail to grow at 35° (Figure 1A). In fact, in all the analyses described in this study, *klp5*Δ and *klp6*Δ cells are phenotypically indistinguishable from the *sot1-1* and *sot2-1* mutant cells, and as a result, *scd1*Δ *klp5*Δ and *scd1*Δ *klp6*Δ cells are phenotypically similar to *scd1*Δ *sot1-1* and *scd1*Δ *sot2-1* cells.

Klp5 and Klp6 specifically interact with the Ras1-Scd1 pathway, but not with the Ras1-Byr2 pathway: *S. pombe* Ras1 controls two effectors. In addition to Scd1, Ras1 also controls the Byr2 protein kinase. We investigated which Ras1 pathway specifically interacts with Klp5 and Klp6. Our data show that at 35°, *ras1*Δ, *scd2*Δ (data not shown), *orb2-34* (a *shk1* mutation; Verde *et al.* 1998), and overexpression of the dominant negative Cdc42T17N inhibit the growth of *klp5*Δ cells; by contrast, deleting *byr2* has no effect on the phenotype of *klp5*Δ cells (Figure 1B). Similar results were observed in *klp6*Δ cells (data not shown). We conclude that the Ras1-Scd1 pathway, but not the Ras1-Byr2 pathway, interacts with the Klp5-Klp6 complex.

To further analyze the relationship between Klp5/6 and the Ras1 pathway, we determined that *klp5* or *klp6* overexpression does not detectably rescue the phenotype of *scd1*Δ and *ras1*Δ cells (round cell shape); conversely, *scd1* or *ras1* overexpression does not rescue the phenotype of *klp5*Δ or *klp6*Δ cells (bent cell shape and sporulation abnormalities; West *et al.* 2001; data not shown). Collectively, these genetic data suggest that the Ras1 pathway and Klp5/6 act in a cooperative fashion, perhaps on different mechanisms, to influence cell growth.

Furthermore, we found that *klp5*Δ and *klp6*Δ do not detectably alter the localization of Scd1 and vice versa (data not shown). Interestingly, in interphase, Scd1 is predominantly nuclear, while Klp5 associates with microtubules. However, when Klp5 is overexpressed, Scd1 seems to relocate from the nucleus to the cytosol as long cables (Figure 1C). These cables are almost certainly microtubules since they are readily demolished by MBC (Figure 1C) and by ice treatment (not shown), both of which induce microtubule depolymerization, but not by latrunculin A (not shown), which induces F-actin depolymerization. These observations suggest that Klp5 overexpression recruits Scd1 to microtubules. By contrast, Scd1 overexpression did not cause Klp5 to mislocalize (data not shown). We conclude that, although components of the Ras1 pathway and Klp5/6 are not necessary for one another's proper cellular localization, high levels of Klp5 can mislocalize Scd1.

Klp5 and Klp6 influence the same biological processes but are not functionally redundant: The Klp5 and Klp6 amino acid sequences are very similar, and we and others have observed that *klp5*Δ and *klp6*Δ cells have similar phenotypes; furthermore, Klp5 and Klp6 can form a protein complex (see below and Garcia *et al.* 2002b). Thus, we asked whether Klp5 and Klp6 are functionally redundant with respect to the interaction with Scd1. A *klp5*Δ *klp6*Δ strain was created, which, like the single null mutants, is viable at all temperatures tested (Figure 1A; West *et al.* 2001). The phenotype of the double null mutant is essentially the same as that of either one of the single null mutants (West *et al.* 2001; data not shown). In addition, the phenotype of a triple null mu-

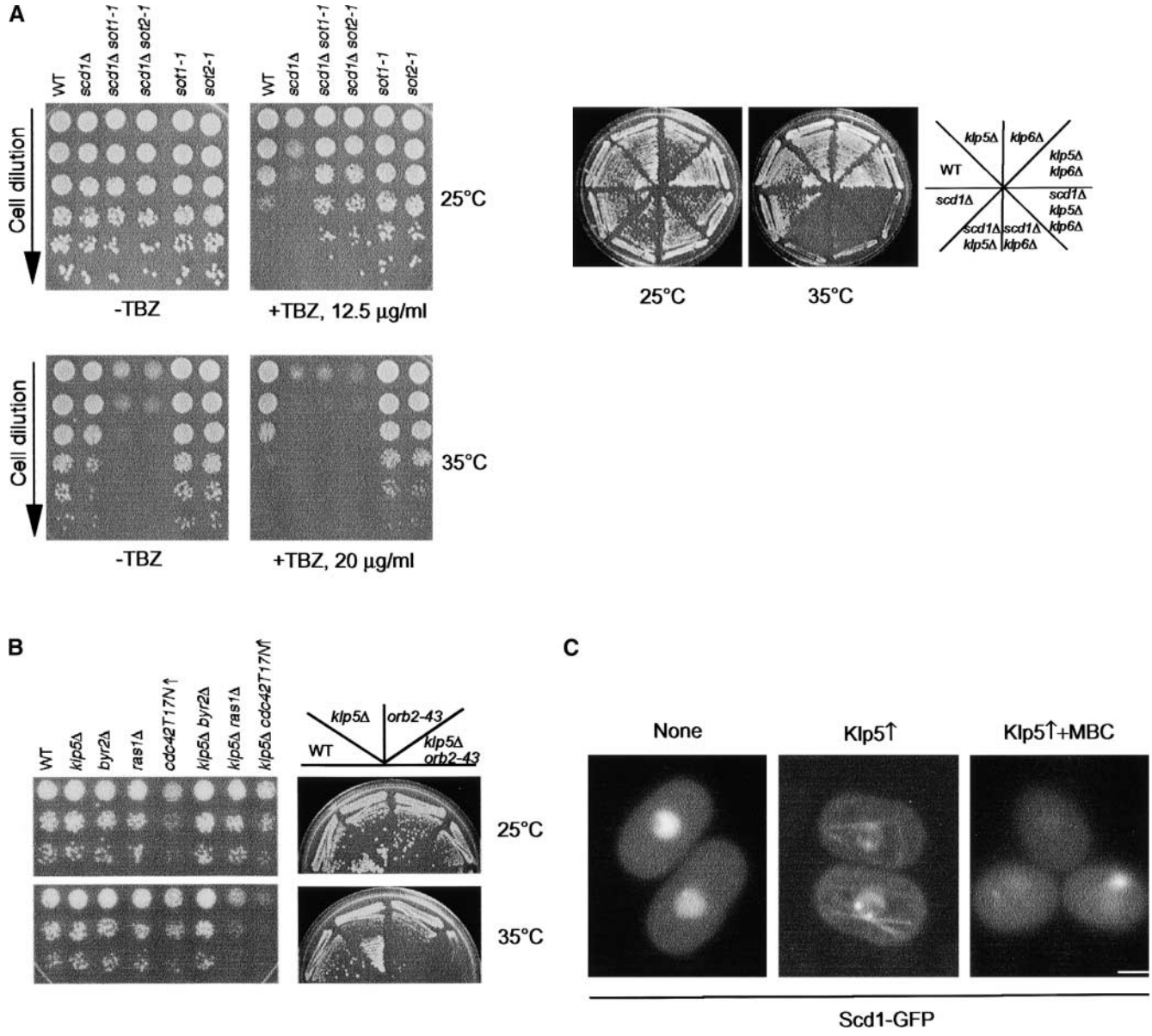

FIGURE 1.—Mutations inactivating *klp5* or *klp6* create a growth defect in cells defective specifically in the Ras1-Scd1 pathway. (A) Serially diluted cells were spotted onto YEAU plates. These plates were incubated at either 25° for 4 days or 35° for 2 days; the amount of TBZ in these plates is indicated. The deletion and wild strains used were SP870 (WT), KLP5U (*klp5*Δ), KLP6U (*klp6*Δ), SCD1L (*scd1*Δ), K5AK6U (*klp5*Δ *klp6*Δ), S1LK5U (*scd1*Δ *klp5*Δ), S1LK6U (*scd1*Δ *klp6*Δ), and S1LK5AK6U (*scd1*Δ *klp5*Δ *klp6*Δ). (B) Cells with indicated gene deletion (Δ) or overexpression (↑) were serially diluted and spotted onto YEAU plates. Plates were cultured at 25° for 3 days or at 35° for 2 days. Strains used were SP870 (WT), KLP5U (*klp5*Δ), SPSL (*byr2*Δ), SPRU (*ras1*Δ), SP42N17 (*cdc42T17N*↑), B2LK5U (*klp5*Δ *byr2*Δ), R1UK5A (*klp5*Δ *ras1*Δ), and K5U42T17N (*klp5*Δ *cdc42T17N*↑). To determine genetic interaction between the *shk1* mutation (*orb2-43*) and *klp5*Δ, the *orb2-43* mutant was fused with strain KLP5A and tetrads were dissected. The four strains shown were derived from the same tetrad. (C) Wild-type cells were transformed with pREP1-SCD1GFP to express Scd1-GFP. MBC was added at 25 μg/ml. Klp5 was further overexpressed (↑) in these cells using pSLF173-KLP5. The thiamine concentration was 0.25 μM. Note that Scd1 overexpression can cause round cell shape. WT, wild type. Bar, 3 μm.

tant lacking *scd1, klp5,* and *klp6* is not substantially different from that of *scd1*Δ *klp5*Δ and *scd1*Δ *klp6*Δ cells (Figure 1A; data not shown); neither Klp5 overexpression in *scd1*Δ *klp6*Δ cells nor Klp6 overexpression in *scd1*Δ *klp5*Δ cells rescues the growth defect (Figure 2A). Klp5 and Klp6 also do not influence each other's association with microtubules since Klp5 seems to associate efficiently with microtubules in *klp6*Δ cells and vice versa (Figure 2B; data not shown). These data support the hypothesis that Klp5 and Klp6 are part of the same protein complex that regulates the same set of biological functions, which include the interaction with Scd1. This

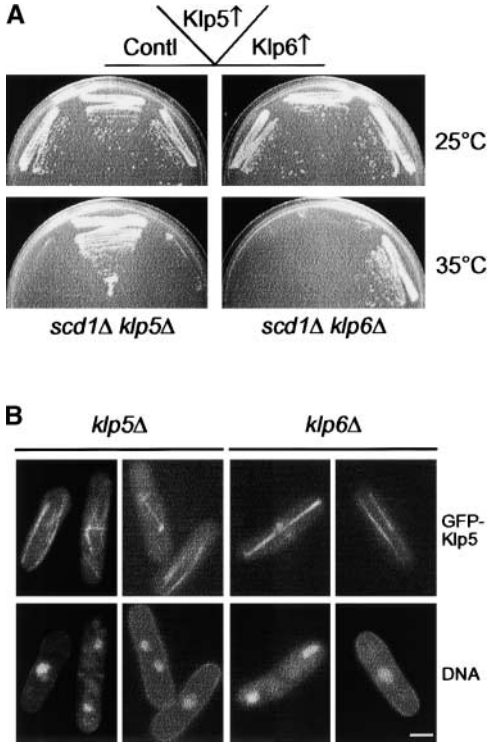

FIGURE 2.—Klp5 and Klp6 act on the same pathway but are not functionally redundant. (A) Cells were transformed with either the control vector (pSLF173) or a vector expressing Klp5 (pSLF173-KLP5) or Klp6 (pSLF173-KLP6). Transformed cells were grown in MM medium with 200 nM thiamine at either 25° for 5 days or 35° for 3 days. We have tried various concentrations of thiamine (0–20 μM) but Klp5 overexpression never rescued *klp6*Δ cells and vice versa. Similar results were obtained by expressing Klp5 and Klp6 under their own genomic promoters (data not shown). (B) Cells were transformed with a vector expressing GFP-Klp5 (pREP41GFP-KLP5) and cultured in MM medium without thiamine. GFP-Klp5 fully rescues the null mutant phenotype and is not toxic to the cell under this condition. Note that treatments of cells with MBC and an ice bath, both of which induce microtubule depolymerization, abolish the GFP-Klp5 signal. GFP tagging of endogenous Klp5 and Klp6 also shows that they localize to microtubules and the spindle (WEST *et al.* 2001). Strains used were KLP5U (*klp5*Δ), KLP6U (*klp6*Δ), S1LK5A (*scd1*Δ *klp5*Δ), and S1LK6A (*scd1*Δ *klp6*Δ). Bar, 3 μm.

complex is apparently inactive when either Klp5 or Klp6 is absent, and Kp5 and Klp6 are not functionally redundant when overexpressed.

Scd1, as well as Cdc42, binds Klp5 and Klp6: We first performed the yeast two-hybrid assay to determine whether Scd1 can bind Klp5 and Klp6. Our data indicate that Scd1 forms stable complexes with Klp5 and with Klp6 (Figure 3A). Klp5 binds Klp6 and itself, while Klp6 binds only Klp5 (Figure 3A). These data agree with those of GARCIA *et al.* (2002b) that Klp5 co-immunoprecipitates with Klp6, but Klp6 does not co-immunoprecipitate with itself in *S. pombe* cells. To examine whether Scd1 forms a stable complex with Klp5 and Klp6 in *S. pombe* cells, we performed GST pull-down. As shown in Figure 3B, Scd1 binds both Klp5 and Klp6. Moreover, like Scd1, Cdc42 binds both Klp5 and Klp6 when expressed in *S. pombe* cells (Figure 3B). The binding between Cdc42 and Klp5/6 does not appear to be GTP dependent since either wild type or the hyperactive form of Cdc42 binds equally efficiently with Klp5/6 (data not shown). Ras1, Scd2, or Shk1 did not show detectable binding with Klp5 and Klp6.

We have shown previously that the C terminus of Scd1 (Scd1ΔN) is central for binding to a number of key molecules, such as Ras1, Scd2, and Cdc42 (CHANG *et al.* 1994). A key feature in the C terminus of Scd1 is a PB1 (*P*hox and *B*em1) domain that adopts a β-grasp fold common among Ras effectors (http://smart.embl-heidelberg.de/smart). We investigated in this study whether the C terminus of Scd1 is also important for binding Klp5 and Klp6 by using the two-hybrid system. As shown in Figure 3C, Scd1ΔN indeed binds both Klp5 and Klp6, albeit it does so more weakly than does full-length Scd1. In contrast, a C-terminally truncated Scd1, Scd1ΔB, lacking just the last 19 amino acids, which are part of the PB1 domain, does not bind Klp5 and Klp6, although it binds the Scd2 control (CHANG *et al.* 1994; data not shown). Scd1ΔB also does not bind Cdc42 and Ras1 (data not shown).

To determine if C-terminal truncation weakens Scd1 function in *S. pombe* cells, we truncated Scd1 by inserting the coding sequence of the c-Myc epitope along with a stop codon (MATERIALS AND METHODS) in the chromosomal coding sequence of *scd1* to result in the production of Scd1ΔB. Western blotting showed that Scd1ΔB and Scd1 are both expressed at the same level (Figure 3D), but cells carrying Scd1ΔB instead of Scd1 are slightly more round than normal (data not shown), suggesting that Scd1ΔB is not as functional as Scd1. More important, *scd1ΔB* also induced Ts growth defects in combination with either *klp5*Δ or *klp6*Δ, although these growth defects are weaker than those created by *scd1*Δ (Figure 3D; data not shown). Collectively, these data suggest that the C terminus of Scd1 is critical for its functions, which includes the interaction with Klp5 and Klp6.

Klp5/6 interact with Scd1 to influence cytokinesis/septation: To determine whether the Ts growth defect of the double mutants is due to cell death or growth inhibition, and to determine its cause, we grew various stains at 25° and then shifted and examined them at 35° over time. We measured cell viability of logarithmically growing cells and found that the viability of *scd1*Δ *klp5*Δ cells declined readily 3 hr after the shift to 35° and then leveled off at 60% (Figure 4A). This observation is consistent with the possibility that a given portion, but not all, of the double-mutant cells loses viability during each cell division. We further observed that multinucleated (two nuclei or more) double-mutant cells with abnormal septa accumulated over time after the shift to 35° (Figure 4B). The observed abnormal septa are either mispositioned (off center) or irregular in shape or both. Strikingly, after 23 hr at 35°, half the

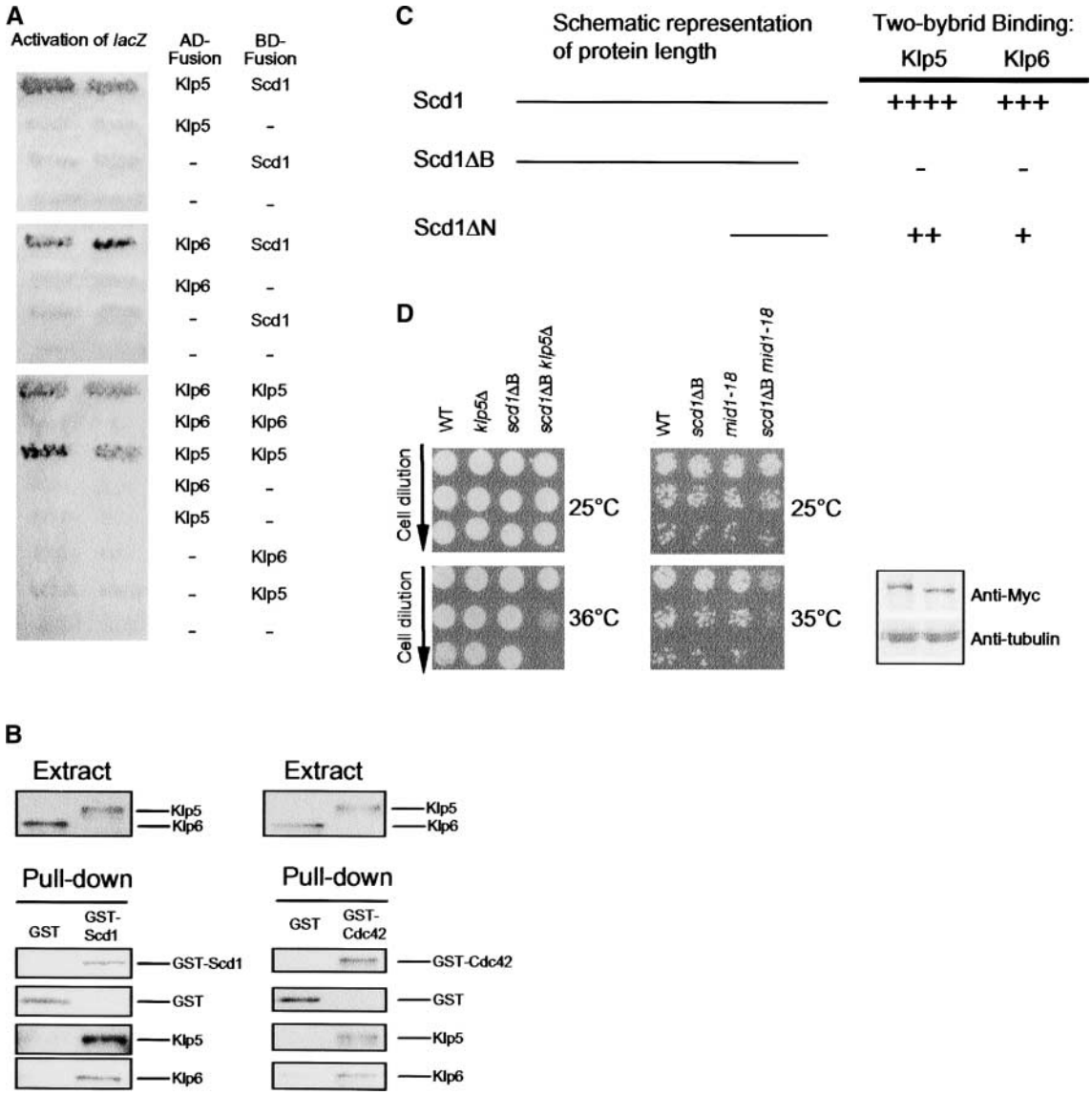

FIGURE 3.—Scd1, as well as Cdc42, binds Klp5 and Klp6. (A) The fusion proteins tested in the two-hybrid system are indicated on the right. AD represents the fusion with the activation domain, while BD represents the fusion with the DNA-binding domain. The activation of the *lacZ* reporter was measured by a color filter assay. The *HIS3* reporter gene was also activated by the same pair of fusion proteins (data not shown). The plasmids expressing the fusion proteins were pGADKLP5, pGADKLP6, pLBDKLP5, pLBDKLP6, and pLBDSCD1. (B) GST control and GST fusion proteins, bound to the glutathione beads and shown on top of each lane, were incubated with yeast lysate containing HA-Klp5 or HA-Klp6. Proteins pulled down by the beads were analyzed by Western blot. HA-Klp5 and HA-Klp6 in the total cell extract were also revealed by Western blot. (C) The yeast two-hybrid interactions between Klp5/6 and various forms of Scd1 were schematized. The plasmids used were pGADKLP5, pGADKLP6, pGAD-SCD1ΔN (CHANG *et al.* 1994), pLBDSCD1ΔB, pLBDSCD1ΔN, pLBDSCD1, and pLBDKLP5. All two-hybrid interactions were determined by activation of both *lacZ* and *HIS3* reporter genes. The interaction between Scd1ΔN and Klp6 was weak and can be detected only by streaking cells transformed with pGADKLP6 and pLBDSCD1ΔN in His^- medium in the presence of 0.5 mM 3-amino-1,2,4-triazole. (D) Serially diluted cells were spotted onto YEAU plates and grew at the indicated temperatures. The strains shown on the left were SP870 (WT), KLP5A (*klp5*Δ), YC2 (*scd1ΔB*), YC4 (*klp5*Δ *scd1ΔB*). All the cells shown on the right were derived from the same tetrad after a fusion between strains YC2 and YDM296. The protein levels of Scd1 and Scd1ΔB were detected by Western blotting, as shown on the right, and tubulins were the loading control.

population of cells are multinucleated, of which 70% have more than two nuclei. The *scd1 klp6* mutants show essentially the same defect (Figure 4B; data not shown). This defect is either undetectable in wild-type, *klp5*Δ, and *klp6*Δ cells or much weaker in *scd1*Δ cells (displaying one-third as many abnormal cells as the double mutants). These observations support the hypothesis that Scd1 and Klp5/6 cooperate to influence cytokinesis and/or septation.

Although Scd1, Klp5, and Klp6 can affect chromosome segregation (LI *et al.* 2000; GARCIA *et al.* 2002b; WEST *et al.* 2002), chromosome missegregation is un-

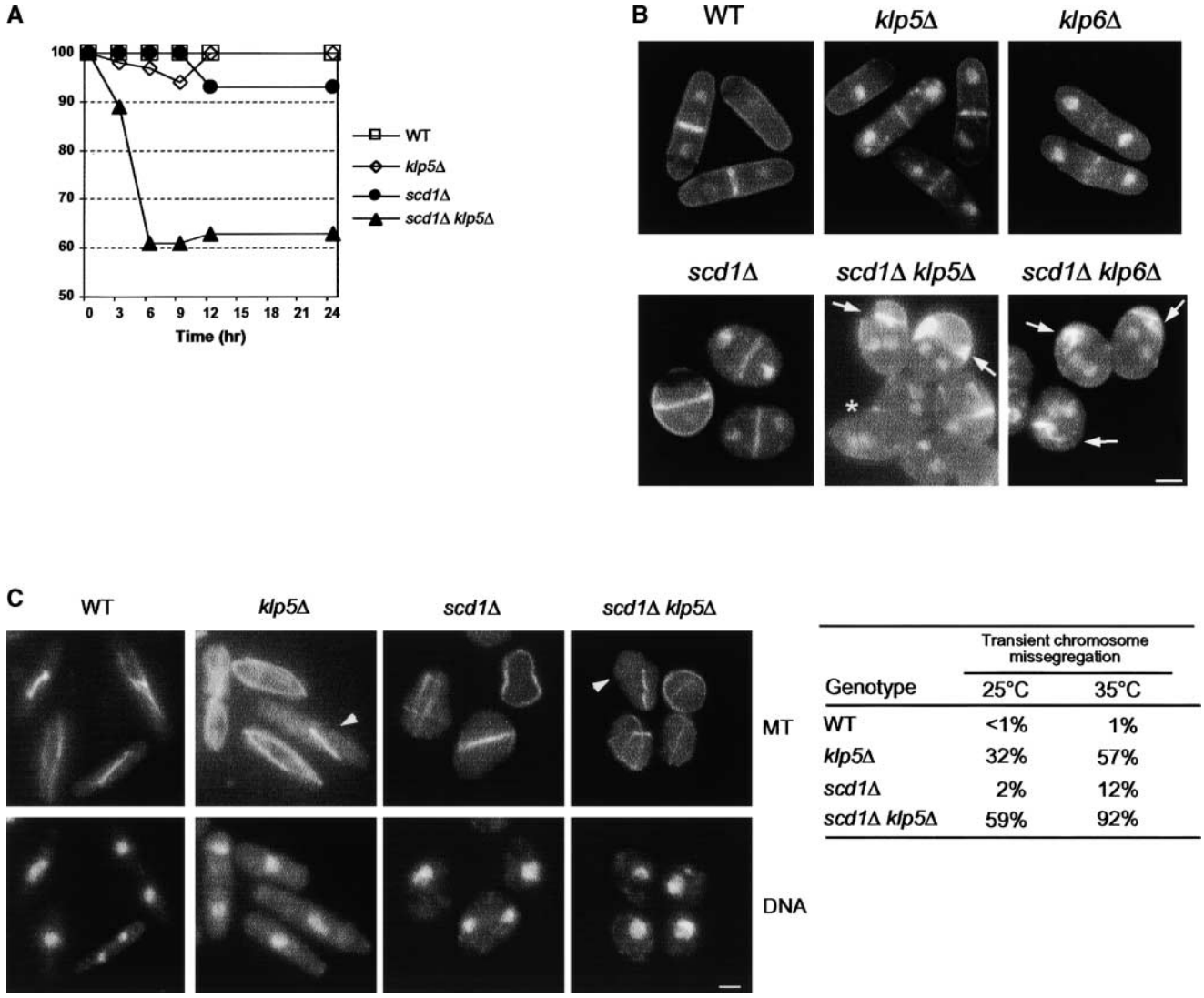

Genotype	Transient chromosome missegregation 25°C	35°C
WT	<1%	1%
*klp5*Δ	32%	57%
*scd1*Δ	2%	12%
*scd1*Δ *klp5*Δ	59%	92%

Figure 4.—Inactivation of both Scd1 and either Klp5 or Klp6 results in abnormal cytokinesis and loss of viability. Strains used were SP870 (WT), KLP5U (*klp5*Δ), KLP6U (*klp6*Δ), SCD1L (*scd1*Δ), S1LK5U (*scd1*Δ *klp5*Δ) and S1LK6U (*scd1*Δ *klp6*Δ). WT, wild type. (A) Cells were pregrown at 25° and then shifted to 35°. Cell samples were taken every 3 hr to determine cell viability by plating. (B) The same samples in A were stained to reveal the septum and DNA. Arrows mark abnormal septa at the same focal plane, while the asterisk marks a four-nucleated cell. (C) Cells pregrown at 25° were shifted to 35° for 4 hr and then stained for microtubules and DNA. Arrowheads mark those cells with unsegregated chromosomes. The frequencies of mitotic cells with abnormal chromosome segregation before and after the shift to 35° are tabulated below. Bars in B and C are 3 μm.

likely to be the major cause of cell death in *scd1*Δ *klp5*Δ and *scd1*Δ *klp6*Δ strains. *klp5*Δ and *klp6*Δ cells with transient unsegregated or lagging chromosomes (arrow heads in Figure 4C) have been reported to occur during anaphase (Garcia *et al.* 2002b; West *et al.* 2002) at both 25° and 35°, but these cells are viable because they apparently were capable of segregating all the chromosomes eventually. The abnormality in chromosome segregation seems to be worsened slightly by *scd1*Δ at 25° and only weakly intensified at 35°. More importantly, at 35°, we did not observe accumulation of double null mutant cells with the "cut" (*c*ell *u*ntimely *t*orn) phenotype that is typical of dead cells resulting from chromosome missegregation. For example, the abnormal cells as shown in Figure 4B have nuclei of equal size. This suggests that the observed lagging chromosomes eventually segregated and that chromosome missegregation is not the major cause for lethality in the double-mutant cells. We also did not observe any obvious defects in microtubules that can explain the cytokinesis phenotype. That is, like *scd1*Δ cells (Pichová *et al.* 1995; Chen *et al.* 1999), the interphase microtubules in the double mutants show a crisscross pattern (Figure 4C). Finally, consistent with the hypothesis that Klp5/6 interacts with the Ras1-Scd1 pathway, inactivation of Ras (*ras1*Δ), Scd2 (*scd2*Δ), Cdc42 (Cdc42T17N overexpression), and Shk1 (*orb2-34*), together with either *klp5*Δ or *klp6*Δ, create a cytokinesis defect similar to that shown in Figure 4B.

Klp5/6 interacts with Scd1 to affect F-actin ring formation and proper Mid1 positioning within the cell cortex: The "septa" as shown in Figure 4B are grossly deformed. Thus, we investigated whether the formation of the contractile ring is defective in the double mutants. To this end, we examined two key ring components, F-actin and Mid1. The former is part of the actomyosin ring, which constricts to cleave the cell, while the latter appears to play a role in marking the site of ring formation.

Our data show that ~60–70% of mitotic *scd1*Δ *klp5*Δ cells displayed either misplaced or disorganized F-actin "rings" or both within the first 3 hr after the shift to 35° (Figure 5A). Most of the disorganized F-actin rings are not closed rings and appear as long threads. Similar abnormalities in F-actin rings are observed in *scd1*Δ *klp6*Δ cells (Figure 5A; data not shown). The observed F-actin abnormalities are similar to those found in mutant cells defective in Mid1 (Chang *et al.* 1996; Bähler *et al.* 1998a).

The subcellular localization of Mid1 was examined by tagging chromosomal Mid1 with 13 copies of the c-Myc epitope. Previous studies have shown that Mid1-Myc is fully functional and is nuclear in wild-type cells during interphase (Bähler *et al.* 1998a; Figure 5B). During early mitosis, Mid1 exits the nucleus and associates with the cell cortex to form a broad band at the cell equator. This band then narrows to form a ring during metaphase-early anaphase. Like F-actin, the Mid1 cortex signal is grossly disorganized and positioned off center in 70% of mitotic *scd1*Δ *klp5*Δ cells after shifting to 35° (Figure 5B). By contrast, this abnormality is undetectable in wild-type and *klp5*Δ cells and can be seen in only 18% of *scd1*Δ cells. Moreover, we found that the percentage of cells with abnormal Mid1 correlates with that of cells with abnormal F-actin ring and that F-actin is almost always associated with Mid1, even when Mid1 is grossly disorganized. We did not detect any significant change of Mid1 localization in interphase *scd1*Δ *klp5*Δ cells; it remains nuclear. Consistent with the idea that Scd1 can influence Mid1 positioning, *scd1*Δ, as well as *scd1*Δ*B*, intensifies the growth defect of the *mid1-18* mutant (Figure 3D). *klp5*Δ and *klp6*Δ do not interact with this *mid1* allele, however.

To further determine the timing of Mid1 and F-actin mislocalization, *scd1*Δ *klp5*Δ cells were synchronized in S phase (by hydroxyurea) at 25° and then released at 35° and allowed to complete the first cell cycle. We found that abnormal Mid1 and F-actin cortex signals can be detected as early as the prometaphase, a stage when Mid1 is normally expected to form a band (data not shown). Therefore, it seems unlikely that the abnormal Mid1 rings are broken-down structures from preformed bands or rings. On the basis of these data, we conclude that Mid1 and F-actin are improperly positioned in the cell cortex when both Scd1 and Klp5/6 are inactivated.

DISCUSSION

This study uncovers a novel function for both the Klp5-Klp6 complex and the Ras1-Scd1 pathway in that they act in concert to mediate cytokinesis. This is supported by the fact that Klp5/6 can form a complex with both Scd1 and Cdc42; furthermore, inactivation of Klp5/6 together with inactivation of the Ras1-Scd1 pathway leads to abnormal cytokinesis. The abnormal cytokinesis appears to be caused by improper contractile ring formation, as the double-mutant cells frequently contain F-actin and Mid1 rings that are either mispositioned or fragmented in the cell cortex.

How the contractile ring is positioned during mitosis is unclear. Using GFP tagging, Mid1 can be observed to associate with the cell cortex as early as in G_2 (Paoletti and Chang 2000). As such, among all the proteins known to influence cytokinesis, Mid1 seems to be the earliest to reach the cell equator. This supports the hypothesis that Mid1 plays a critical role in recruiting other cytokinesis elements to the cell equator. Since Mid1 is grossly mispositioned in our double mutants, it is tempting to speculate that Mid1 mispositioning may initiate the formation of abnormal F-actin rings. Alternatively, Scd1 and Klp5/6 may influence other proteins, which in turn control Mid1 localization. Mid1 localization can be influenced by Plo1, a Polo-like protein kinase (Bähler *et al.* 1998a). By GFP tagging, Plo1 has been reported to associate with the cell equator briefly during mitosis. We were unable to thoroughly investigate whether Plo1 localization is similarly impaired in our double mutants because GFP-Plo1 loses fluorescence at 35° (our unpublished observation).

Klp5 and Klp6 are presumptive kinesin motors; thus, they are likely to influence cytokinesis in a microtubule-dependent fashion and may act as plus-end motors to play a role in transporting cytokinesis regulatory proteins. Klp5 and Klp6 have also been suggested to play a role in negatively regulating microtubule dynamics, as microtubules in the null mutants are resistant to drugs (TBZ and MBC) that promote microtubule depolymerization and appear so long that they curve within the cell (West *et al.* 2001). Enhancement in apparent microtubule dynamics *per se* is unlikely to cause the observed cytokinesis defects in the *scd1* and *klp* double mutants. This is supported by two of our lines of results: (1) MBC and TBZ resistance in the *scd1 klp* double mutants is actually weaker than that in the *klp* single mutants and (2) adding TBZ and deleting *mal3* (Beinhauer *et al.* 1997), both of which weaken microtubules, did not rescue the growth defect in *scd klp* double mutants. Microtubule dynamics can influence nucleus positioning (Tran *et al.* 2001). While we observed that the nuclei in some of the *klp* mutants cells (5–10%) are off center, this is unlikely to cause the observed Mid1 abnormalities for two reasons:

1. In studies in which a correlation between nucleus

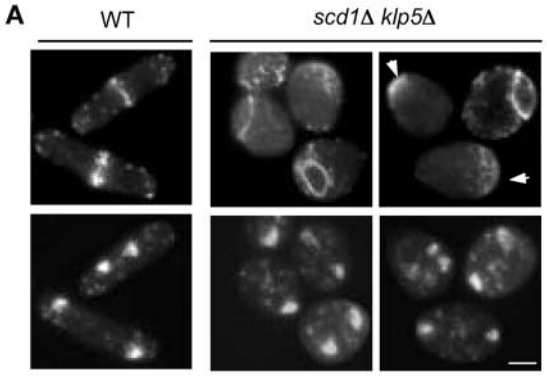

Relevant genotype	% of abnormal mitotic F-actin signal after shift to 35°C over time (hr)			
	0	3	6	9
WT	<1	<1	<1	<1
klp5Δ	<1	3	6	<1
klp6Δ	<1	<1	3	5
scd1Δ	3	32	35	29
scd1Δ klp5Δ	17	68	80	79
scd1Δ klp6Δ	25	59	68	85

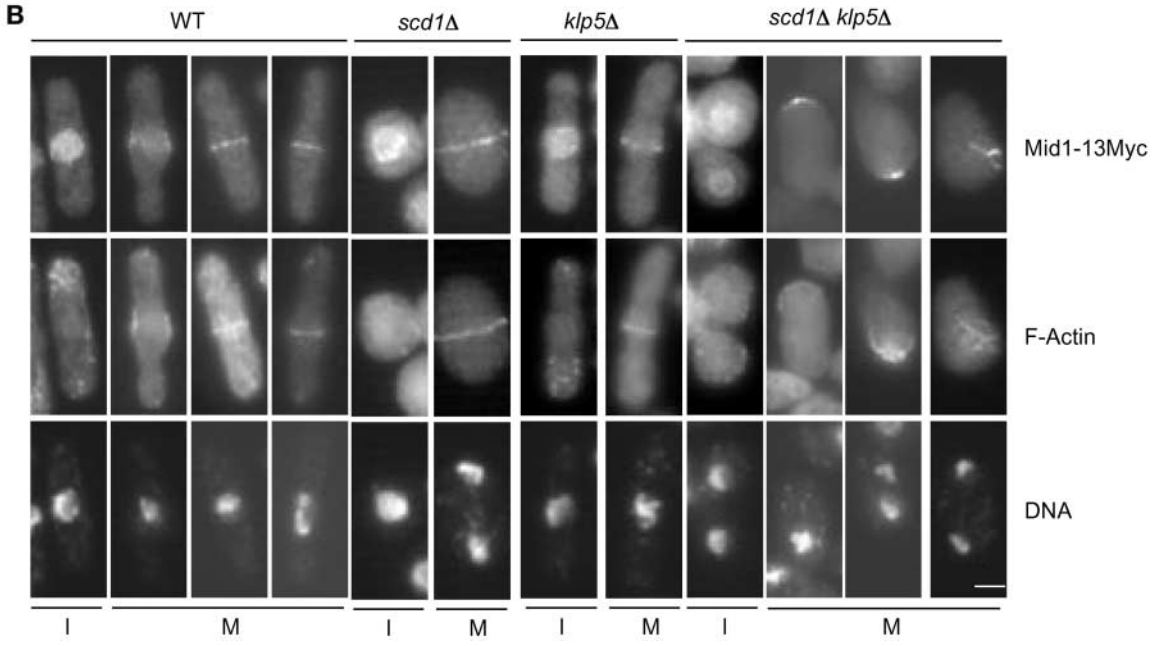

FIGURE 5.—Inactivation of both Scd1 and either Klp5 or Klp6 interferes with F-actin ring formation and Mid1 cortex association. (A) Cells were treated as described in the legend for Figure 4 and then stained for F-actin and DNA. Arrows mark the disorganized F-actin associated with cell ends in mitotic cells. The percentages of mitotic cells with abnormal F-actin were also tabulated. Bar, 5 μm. (B) Cells were shifted to 35° for 4 hr and then stained for c-Myc, F-actin, and DNA. I, interphase; M, mitosis. Among those mitotic cells with Mid1 in the cortex, we measured the fraction of these cells in which the association between Mid1 and the cell cortex was abnormal. At 35°, this abnormality was 70% in *scd1*Δ *klp5*Δ cells. By contrast, it was 18% in *scd1*Δ cells and <1% in either *klp5*Δ or wild-type cells. At 25°, this abnormality was detectable only in 4% of mitotic *scd1*Δ *klp5*Δ cells, but not in the wild type or in any of the single null mutants. About 1000 synchronized cells were counted for each strain. Bar, 3 μm.

mispositioning and abnormal F-actin ring formation has been noted, the F-actin ring seems to be assembled normally but is simply positioned off center in relation to the nucleus (CHANG *et al.* 1996). In our double mutants, by contrast, most of the abnormal F-actin does not form a ring at all and is grossly disorganized in the cortex. This abnormality resembles that of the *mid1* mutant, whose nucleus is not misplaced.

2. We examined those *scd1*Δ *klp5*Δ cells that are not entirely spherical and found that there is barely a 2-fold increase in the fraction of off-centered nuclei after shifting to 35° (our unpublished results). By contrast, the increase in abnormal Mid1 is >10-fold.

Interacting with microtubule-binding proteins to influence cytokinesis seems to be a common feature of the Ras1-Scd1 pathway, as we have previously reported that it can do so with Tea1 (PAPADAKI *et al.* 2002), and in this study we show that it also does so with Klp5/6. Furthermore, in ongoing studies, we found that *scd1*Δ together with *mal3*Δ also causes a cytokinesis defect (our unpublished results). How does the Ras1-Scd1 pathway influence cytokinesis? There is evidence that the Ras1-Scd1 pathway can affect protein trafficking. MURRAY and JOHNSON (2000a) have demonstrated that this Ras1 pathway plays a role in endocytic trafficking, and we have shown that it controls the nuclear import of Moe1 and Rpn5 (CHEN *et al.* 1999; YEN *et al.* 2003). These

observations support a hypothesis that the Ras1-Scd1 pathway may influence nuclear localization of key cytokinesis regulators. Alternatively, the Ras1 pathway may influence cytokinesis by anchoring regulatory proteins to the potential cleavage site. One prediction of this model is that components of the Ras1 pathway can associate with the cell midzone. Indeed, during early mitosis Scd2 forms a wide band around the cell equator (Sawin and Nurse 1998), which is very similar in appearance to the Mid1 band; furthermore, Ras1, Scd1, Cdc42, and Shk1 all associate with the cell equator (Bauman *et al.* 1998; Li *et al.* 2000; Murray and Johnson 2000b; Qyang *et al.* 2002). Finally, the Ras1 pathway may interact with the SIN pathway, a key signal transduction pathway that regulates cytokinesis (McCollum and Gould 2001). In keeping with this, overexpression of a negative regulator for the SIN pathway (Byr4) can block cytokinesis, which is worsened by *ras1*Δ and *scd1*Δ (Song *et al.* 1996).

In both plant and animal cells, microtubules and, in particular, kinesin motor proteins are very important for cytokinesis (Smith 2002). In *S. pombe*, the roles of microtubules in cytokinesis are somewhat less well defined, although they have been implicated in cytokinesis in at least two other studies. It has been shown that Mal3 overexpression can cause abnormal septum formation (Beinhauer *et al.* 1997) and that Cdc12, a crucial component for proper cytokinesis, associates with microtubules (Chang 1999). One paradoxical observation questions the importance of microtubules in cytokinesis. That is, a β-tubulin mutant can still form an F-actin ring in the cold when almost all long microtubule cables are presumed to depolymerize (Chang *et al.* 1996). How can Klp5 and Klp6 function in this mutant if in fact all microtubules undergo depolymerization? Our genetic data suggest that Scd1 and the Klp5-Klp6 complex may engage in two different mechanisms that ultimately converge upon cytokinesis control. In the absence of a normal microtubule cytoskeleton, Scd1 may act through pathways that are sufficient in the cold to support localization of cytokinesis regulators. Furthermore, it has been shown that GFP-Mid1 associates with the cell cortex as early as in G_2 and that, once in the cell cortex, the positioning of GFP-Mid1 is resistant to microtubule depolymerization (Paoletti and Chang 2000). Thus, even if Mid1 localization is only weakly supported by Scd1 in the absence of microtubules, once Mid1 reaches the cell cortex, it could stay there until cell division. We were unable to test whether the Mid1 band in early G_2 is affected in the *scd1* and *klp* mutants because the GFP signal is unstable at 36° (our unpublished results).

Since the Ras-Cdc42 pathway is highly conserved from yeast to humans, it is possible that this pathway also regulates cytokinesis in other eukaryotic cells. Rho-like proteins, such as Cdc42, have been shown to control cytokinesis in numerous systems, including many animal cells (Lin *et al.* 1999; Prokopenko *et al.* 2000), and Ras can regulate cytokinesis in Dictyostelium (Sutherland *et al.* 2001).

We deeply appreciate D. McCollum, F. Chang, S. Marcus, and F. Verde for providing materials critical for this study and the discussion. We also thank J. Blau and C. Rushlow from New York University for critically reading our manuscript, members of the Chang lab for discussion, and R. West and R. McIntosh for sharing unpublished results on *klp5* and *klp6*. This study was supported by the National Institutes of Health (R01-CA90464) and the Department of Defense (BC021935).

LITERATURE CITED

Alfa, C., P. Fantes, J. Hyams, M. McLeod and E. Warbrick, 1993 *Experiments with Fission Yeast.* Cold Spring Harbor Laboratory Press, Cold Spring Harbor, NY.

Bähler, J., A. B. Steever, S. Wheatley, Y. Wang, J. R. Pringle *et al.*, 1998a Role of polo kinase and Mid1p in determining the site of cell division in fission yeast. J. Cell Biol. **143:** 1603–1616.

Bähler, J., J. Q. Wu, M. S. Longtine, N. G. Shah, A. McKenzie, III, *et al.*, 1998b Heterologous modules for efficient and versatile PCR-based gene targeting in *Schizosaccharomyces pombe.* Yeast **14:** 943–951.

Barbet, N., W. J. Muriel and A. M. Carr, 1992 Versatile shuttle vectors and genomic libraries for use with Schizosaccharomyces pombe. Gene **114:** 59–66.

Bauman, P., Q.-P. Cheng and C. F. Albright, 1998 The Byr2 kinase translocates to the plasma membrane in a Ras1-dependent manner. Biochem. Biophys. Res. Commun. **244:** 468–474.

Beinhauer, J. D., I. M. Hagan, J. H. Hegemann and U. Fleig, 1997 Mal3, the fission yeast homologue of the human APC-interacting protein EB-1 is required for microtubule integrity and the maintenance of cell form. J. Cell Biol. **139:** 717–728.

Chang, E. C., M. Barr, Y. Wang, V. Jung, H. Xu *et al.*, 1994 Cooperative interaction of *S. pombe* proteins required for mating and morphogenesis. Cell **79:** 131–141.

Chang, E., G. Bartholomeusz, R. Pimental, J. Chen, H. Lai *et al.*, 1999 Direct binding and *in vivo* regulation of the fission yeast PAK Shk1 by the SH3 domain protein Scd2. Mol. Cell. Biol. **16:** 8066–8077.

Chang, F., 1999 Movement of a cytokinesis factor cdc12p to the site of cell division. Curr. Biol. **9:** 849–852.

Chang, F., A. Woolland and P. Nurse, 1996 Isolation and characterization of fission yeast mutants defective in the assembly and placement of the contractile actin ring. J. Cell Sci. **109:** 131–142.

Chen, C.-R., Y.-C. Li, J. Chen, M. C. Hou, P. Papadaki *et al.*, 1999 Moe1, a novel conserved protein in *Schizosaccharomyces pombe*, interacts with a Ras effector, Scd1, to affect proper spindle formation. Proc. Natl. Acad. Sci. USA **96:** 517–522.

Forsburg, S. L., and D. A. Sherman, 1997 General purpose tagging vectors for fission yeast. Gene **191:** 191–195.

Fukui, Y., and Y. Kaziro, 1985 Molecular cloning and sequence analysis of a ras gene from *Schizosaccharomyces pombe.* EMBO J. **4:** 687–691.

Fukui, Y., and M. Yamamoto, 1988 Isolation and characterization of *Schizosaccharomyces pombe* mutants phenotypically similar to *ras1*$^-$. Mol. Gen. Genet. **215:** 26–31.

Garcia, M. A., N. Koonrugsa and T. Toda, 2002a Spindle-kinetochore attachment requires the combined action of Kin I-like Klp5/6 and Alp14/Dis1-MAPs in fission yeast. EMBO J. **21:** 6015–6024.

Garcia, M. A., N. Koonrugsa and T. Toda, 2002b Two kinesin-like Kin I family proteins in fission yeast regulate the establishment of metaphase and the onset of anaphase A. Curr. Biol. **12:** 610–621.

Gilbreth, M., P. Yang, D. Wang, J. Frost, A. Polverino *et al.*, 1996 The highly conserved *skb1* gene encodes a protein that interacts with Shk1, a fission yeast Ste20/PAK homolog. Proc. Natl. Acad. Sci. USA **93:** 13802–13807.

Kim, H. W., P. Yang, Y. Qyang, H. Lai, H. Du *et al.*, 2001 Genetic and molecular characterization of Skb15, a highly conserved inhibitor of the fission yeast PAK, Shk1. Mol. Cell 7: 1095–1101.

Li, Y.-C., C.-R. Chen and E. C. Chang, 2000 Fission yeast Ras1

effector Scd1 interacts with the spindle and affects its proper formation. Genetics **156:** 995–1004.

Lin, R., R. A. Cerione and D. Manor, 1999 Specific contributions of the small GTPases Rho, Rac, and Cdc42 to Dbl transformation. J. Biol. Chem. **274:** 23633–23641.

Marcus, S., A. Polverino, E. Chang, D. Robbins, M. H. Cobb *et al.*, 1995 Shk1, a homolog of the *Saccharomyces cerevisiae* Ste20 and mammalian p65^{PAK} protein kinase, is a component of a Ras/Cdc42 signaling module in the fission yeast, *Schizosaccharomyces pombe*. Proc. Natl. Acad. Sci. USA **92:** 6180–6184.

Mata, J., and P. Nurse, 1997 tea1 and the microtubular cytoskeleton are important for generating global spatial order within the fission yeast cell. Cell **89:** 939–949.

McCollum, D., and K. L. Gould, 2001 Timing is everything: regulation of mitotic exit and cytokinesis by the MEN and SIN. Trends Cell Biol. **11:** 89–95.

Murray, J. M., and D. I. Johnson, 2000a The Cdc42p GTPase and its regulators Nrf1p and Scd1p are involved in endocytic trafficking in the fission yeast S. pombe. J. Biol. Chem. **276:** 3004–3009.

Murray, J. M., and D. I. Johnson, 2000b Isolation and characterization of Nrf1p, a novel negative regulator of the Cdc42p GTPase in *Schizosaccharomyces pombe*. Genetics **154:** 155–165.

Paoletti, A., and F. Chang, 2000 Analysis of mid1p, a protein required for placement of the cell division site, reveals a link between the nucleus and the cell surface in fission yeast. Mol. Biol. Cell **11:** 2757–2773.

Papadaki, P., V. Pizon, B. Onken and E. C. Chang, 2002 Two Ras pathways in fission yeast are differentially regulated by two Ras GEFs. Mol. Cell. Biol. **22:** 4598–4606.

Pichová, A., S. D. Kohlwein and M. Yamamoto, 1995 New arrays of cytoplasmic microtubules in the fission yeast *Schizosaccharomyces pombe*. Protoplasma **188:** 252–257.

Prokopenko, S. N., R. Saint and H. J. Bellen, 2000 Untying the Gordian knot of cytokinesis. Role of small G proteins and their regulators. J. Cell Biol. **148:** 843–848.

Qyang, Y., P. Yang, H. D. Du, H. Lai, H. W. Kim *et al.*, 2002 The p21-activated kinase, Shk1, is required for proper regulation of microtubule dynamics in the fission yeast, Schizosaccharomyces pombe. Mol. Microbiol. **44:** 325–334.

Sawin, K. E., and P. Nurse, 1998 Regulation of cell polarity by microtubules in fission yeast. J. Cell Biol. **142:** 457–471.

Smith, L. G., 2002 Plant cytokinesis: motoring to the finish. Curr. Biol. **12:** 206–208.

Sohrmann, M., C. Fankhauser, C. Brodbeck and V. Simanis, 1996 The dmf1/mid1 gene is essential for correct positioning of the division septum in fission yeast. Genes Dev. **10:** 2707–2719.

Song, K., K. E. Mach, C. Y. Chen, T. Reynolds and C. F. Albright, 1996 A novel suppressor of *ras1* in fission yeast, *byr4*, is a dosage-dependent inhibitor of cytokinesis. J. Cell Biol. **133:** 1307–1319.

Sutherland, B. W., G. B. Spiegelman and G. Weeks, 2001 A Ras subfamily GTPase shows cell cycle-dependent nuclear localization. EMBO Rep. **2:** 1024–1028.

Tran, P. T., L. Marsh, V. Doye, S. Inoue and F. Chang, 2001 A mechanism for nuclear positioning in fission yeast based on microtubule pushing. J. Cell Biol. **153:** 397–411.

Van Aelst, L., and C. D'Souza-Schorey, 1997 Rho GTPases and signaling networks. Genes Dev. **11:** 2295–2322.

Verde, F., D. J. Wiley and P. Nurse, 1998 Fission yeast *orb6*, a ser/thr protein kinase related to mammalian rho kinase and myotonic dystrophy kinase, is required for maintenance of cell polarity and coordinates cell morphogenesis with the cell cycle. Proc. Natl. Acad. Sci. USA **95:** 7526–7531.

Vojtek, A. B., S. M. Hollenberg and J. A. Cooper, 1993 Mammalian Ras interacts directly with the serine/threonine kinase Raf. Cell **74:** 205–214.

Wang, Y., H. P. Xu, M. Riggs, L. Rodgers and M. Wigler, 1991 *byr2*, a *Schizosaccharomyces pombe* gene encoding a protein kinase capable of partial suppression of the *ras1* mutant phenotype. Mol. Cell. Biol. **11:** 3554–3563.

West, R. R., T. Malmstrom, C. L. Troxell and J. R. McIntosh, 2001 Two related kinesins, klp5(+) and klp6(+), foster microtubule disassembly and are required for meiosis in fission yeast. Mol. Biol. Cell **12:** 3919–3932.

West, R. R., T. Malmstrom and J. R. McIntosh, 2002 Kinesins klp5(+) and klp6(+) are required for normal chromosome movement in mitosis. J. Cell Sci. **115:** 931–940.

Yen, H. C., C. Gordon and E. C. Chang, 2003 Schizosaccharomyces pombe Int6 and Ras homologs regulate cell division and mitotic fidelity via the proteasome. Cell **112:** 207–217.

Communicating editor: T. Stearns